Characterization of two novel lipopolysaccharide phosphoethanolamine transferases in Pasteurella multocida and their role in resistance to cathelicidin-2

Harper, Marina; Wright, Amy; St. Michael, Frank; Li, Jianjun; Deveson Lucas, Deanna; Ford, Mark; Adler, Ben; Cox, Andrew D.; Boyce, John D.

Publisher's version / Version de l'éditeur:
https://doi.org/10.1128/IAI.00557-17
Infection and Immunity, 85, 11, 2017-09-05

AMERICAN SOCIETY FOR MICROBIOLOGY | Infection and Immunity®

MOLECULAR PATHOGENESIS

Characterization of Two Novel Lipopolysaccharide Phosphoethanolamine Transferases in *Pasteurella multocida* and Their Role in Resistance to Cathelicidin-2

Marina Harper,[a] Amy Wright,[a] Frank St. Michael,[b] Jianjun Li,[b] Deanna Deveson Lucas,[a] Mark Ford,[c] Ben Adler,[a] Andrew D. Cox,[b] John D. Boyce[a]

Infection and Immunity Program, Monash Biomedicine Discovery Institute and Department of Microbiology, Monash University, VIC, Australia[a]; Vaccine Program, Human Health Therapeutics Portfolio, National Research Council, Ottawa, ON, Canada[b]; CSIRO Australian Animal Health Laboratory, Geelong, VIC, Australia[c]

ABSTRACT The lipopolysaccharide (LPS) produced by the Gram-negative bacterial pathogen *Pasteurella multocida* has phosphoethanolamine (PEtn) residues attached to lipid A, 3-deoxy-D-manno-octulosonic acid (Kdo), heptose, and galactose. In this report, we show that PEtn is transferred to lipid A by the *P. multocida* EptA homologue, PetL, and is transferred to galactose by a novel PEtn transferase that is unique to *P. multocida* called PetG. Transcriptomic analyses indicated that *petL* expression was positively regulated by the global regulator Fis and negatively regulated by an Hfq-dependent small RNA. Importantly, we have identified a novel PEtn transferase called PetK that is responsible for PEtn addition to the single Kdo molecule (Kdo_1), directly linked to lipid A in the *P. multocida* glycoform A LPS. *In vitro* assays showed that the presence of a functional *petL* and *petK*, and therefore the presence of PEtn on lipid A and Kdo_1, was essential for resistance to the cationic, antimicrobial peptide cathelicidin-2. The importance of PEtn on Kdo_1 and the identification of the transferase responsible for this addition have not previously been shown. Phylogenetic analysis revealed that PetK is the first representative of a new family of predicted PEtn transferases. The PetK family consists of uncharacterized proteins from a range of Gram-negative bacteria that produce LPS glycoforms with only one Kdo molecule, including pathogenic species within the genera *Vibrio*, *Bordetella*, and *Haemophilus*. We predict that many of these bacteria will require the addition of PEtn to Kdo for maximum protection against host antimicrobial peptides.

KEYWORDS lipopolysaccharide, phosphoethanolamine transferase, *Pasteurella multocida*, 3-deoxy-D-manno-octulosonic acid, cathelicidin, cationic antimicrobial

Pasteurella multocida is a Gram-negative bacterium present in the nasopharynx of many healthy animals, including domestic cats and dogs. However, when transmitted to susceptible hosts, including birds, cattle, pigs, rabbits, and humans, the bacterium can cause serious joint, soft tissue, and respiratory infections as well as life-threatening septicemia (1, 2). *P. multocida* is the causative agent of acute fowl cholera, a systemic disease of birds that causes significant losses to poultry industries worldwide. Our structural and genetic analyses of the lipopolysaccharide (LPS) produced by a number of *P. multocida* field isolates and historical type strains revealed that a wide range of outer core LPS structures were produced by *P. multocida*; accordingly, strains could be classified into eight different LPS genotypes, L1 to L8 (3–5). Many fowl cholera outbreaks are caused by *P. multocida* serogroup A:L1 strains (capsule type A, LPS genotype L1); these strains produce two major virulence factors that are essential

Received 7 August 2017 **Returned for modification** 24 August 2017 **Accepted** 29 August 2017

Accepted manuscript posted online 5 September 2017

Citation Harper M, Wright A, St. Michael F, Li J, Deveson Lucas D, Ford M, Adler B, Cox AD, Boyce JD. 2017. Characterization of two novel lipopolysaccharide phosphoethanolamine transferases in *Pasteurella multocida* and their role in resistance to cathelicidin-2. Infect Immun 85:e00557-17. https://doi.org/10.1128/IAI.00557-17.

Editor Guy H. Palmer, Washington State University

Address correspondence to Marina Harper, marina.harper@monash.edu.

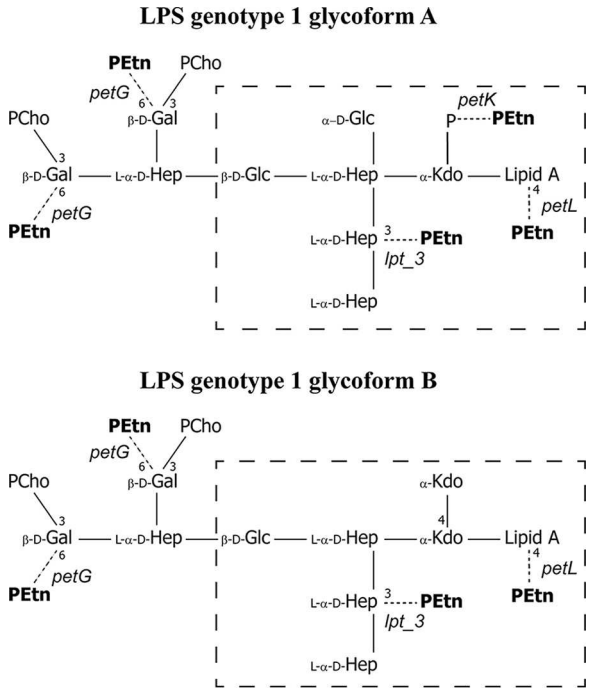

FIG 1 Schematic representation of the two LPS glycoforms, A and B, produced by *P. multocida* strains X73 and VP161 that belong to LPS genotype 1 (Heddleston serotype 1). LPS glycoforms A and B have identical outer core sugars and linkages (not shown) but differ in the inner core (within square) with respect to the number of 3-deoxy-D-manno-oct-2-ulosonic acid (Kdo), glucose, and phosphoethanolamine (PEtn) residues. The addition of phosphoethanolamine (PEtn) is nonstoichiometric, but PEtn may be present at the 4′ position of lipid A, on the phosphorylated Kdo in LPS glycoform A, at the 3 position on the second inner core heptose, and at the 6 position on both galactose residues located at the terminal end of the LPS molecule. Strain VP161 produces LPS glycoforms with PEtn only on lipid A and Kdo-P. Strain X73 produces LPS glycoforms with PEtn on the lipid A, Kdo-P, the second heptose, and the terminal galactose residues. Residues are indicated as follows: β-D-Gal, β-D-galactose; β-D-Glc, β-D-glucose; L-α-D-Hep, L-α-D-heptose; Kdo, 3-deoxy-D-manno-oct-2-ulosonic acid; P, phosphate; PCho, phosphocholine; PEtn, phosphoethanolamine.

for their ability to cause disease in chickens, namely, a hyaluronic acid capsule which confers serum resistance and an L1 LPS (6–9).

The structure of the LPS inner core is conserved across all *P. multocida* strains and contains 3-deoxy-D-manno-oct-2-ulosonic acid (Kdo), heptose (Hep), and glucose (Glu). Unusually, most *P. multocida* strains, including those belonging to LPS genotype L1, simultaneously produce two major LPS glycoforms, A and B, that have identical outer core structures but differ in the inner core region with respect to the number of Kdo residues (one in glycoform A, two in glycoform B) and glucose residues (two in glycoform A, one in glycoform B) and with respect to the number and position of phosphoethanolamine (PEtn) residues (Fig. 1). PEtn is a positively charged moiety that can be added in a nonstoichiometric manner at up to three positions in the *P. multocida* LPS inner core (Fig. 1): to lipid A (at the 4′ position), to the phosphate on the 4 position of Kdo in glycoform A, or to the 3 position of the second Hep (Hep II).

The addition of PEtn to the inner core of the *P. multocida* LPS is predicted to vary according to the strain and to the growth conditions. Capillary electrophoresis–mass spectrometry (CE-MS) analysis of O-deacylated LPS (LPS-OH) isolated from *P. multocida* strain VP161 grown *in vitro* in liquid broth revealed the presence of glycoform B and two glycoforms representing glycoform A, either with or without a PEtn residue attached to the phosphorylated Kdo residue. Analysis of LPS isolated from VP161 cells grown on chocolate blood agar revealed two different lipid A molecules (lipid A-OH species at 952 atomic mass units [amu] and 1,075.0 amu), the larger of which corresponds to lipid A with a PEtn residue attached (3). However, when *P. multocida* strain

VP161 or X73 was grown in liquid broth, no PEtn was detected on the lipid A moiety of the LPS produced by either strain (3, 10).

As *P. multocida* LPS does not contain a repeating O-antigen, the outer core sugars are the most distal part of the LPS molecule. The outer core region of the L1 LPS produced by highly virulent fowl cholera strains VP161 and X73 consists of a single heptose with two galactose (Gal) residues attached at the 4 and 6 positions on the heptose. Each of the two Gal residues in both VP161 and X73 is decorated with phosphocholine (PCho) at the 3 position (3), and the Gal residues are further decorated with PEtn in the LPS produced by strain X73 (Fig. 1) (10).

The transferases responsible for the addition of PEtn to lipid A (EptA) and to the 3 position or 6 position on Hep II in the LPS inner core (Lpt-3 or Lpt-6, respectively) have been identified in other bacteria, including *Haemophilus influenzae* and *Neisseria meningitis* (11, 12). We previously identified an *lpt3* homologue in *P. multocida* and showed that Lpt-3 was responsible for addition of PEtn to the 3 position on Hep II of the *P. multocida* LPS (13). In many strains, however, *lpt3* is present as a pseudogene and Hep II is not decorated with PEtn. Moreover, although strain X73 has a functional *lpt3* gene, X73 cells grown *in vitro* do not elaborate PEtn on Hep II, suggesting that expression of *lpt3* is regulated in response to the environment.

In this study, we used bioinformatic analyses combined with structural and functional assays to identify and characterize three PEtn transferases responsible for PEtn addition to the various positions on the genotype 1 LPS. We identified two novel LPS-associated PEtn transferases, PetG (which is required for the addition of PEtn to the terminal galactose residues in *P. multocida* X-73 LPS) and PetK (which transfers PEtn to Kdo-P), and showed that PetK represents a new family of bacterial PEtn transferases. We also proved that the presence of PEtn on both lipid A and Kdo-P is critical for *P. multocida* to resist killing by the antimicrobial peptide, cathelicidin-2.

RESULTS

Bioinformatic analysis identifies two novel *P. multocida* proteins that belong to the PEtn transferase family. In order to identify novel *P. multocida* PEtn transferases, we used the amino acid sequences of three previously characterized PEtn transferases to query the *P. multocida* genomes. Each of the *lpt3* genes present in *N. meningitis* (Lpt-3_{Nm}/NMB2010) and *P. multocida* (Lpt-3_{Pm}/A0R63_02570) encodes a PEtn transferase that is responsible for addition of PEtn onto the 3 position of Hep II in the LPS inner core (13, 14). *N. meningitidis* gene NMB1638 encodes $EptA_{Nm}$, which transfers PEtn to lipid A (11). These transferases all belong to the sulfatase family of proteins and contain five transmembrane helices, indicative of inner membrane-associated proteins. The amino acid sequences of these PEtn transferases were used to search the genomes of *P. multocida* strains VP161 and X73. In total, three genes were identified in X73 that encoded proteins with significant identity with Lpt-3_{Pm}, Lpt-3_{Nm}, and/or $EptA_{Nm}$, namely, A0R63_03465, A0R63_06305, and A0R63_09570. Each of the encoded products contained predicted sulfatase domains and at least four transmembrane helices. Intact homologs of X73 genes A0R63_06305 and A0R63_09570 were identified in strain VP161 (99% identity). A homologue of A0R63_03465 that shared 99% identity at the nucleotide level was also present in VP161 but was a pseudogene due to a single base deletion at nucleotide 1071.

The amino acid sequences of the characterized *P. multocida* PEtn transferase, Lpt-3_{Pm}, and the newly identified putative *P. multocida* PEtn transferases (X73 locus tags A0R63_03465, A0R63_06305, and A0R63_09570, respectively) were used in a multiple alignment together with all the functionally characterized bacterial PEtn transferases, as well as a number of uncharacterized proteins that shared a high level of identity with one or more of these proteins (see Fig. S1 in the supplemental material). The alignment data were then used to build a phylogenetic tree (Fig. 2). The functionally characterized transferases included three EptA homologs for which the catalytic domain structure has been resolved, namely, $EptA_{Nm}$ (LptA) (15) and the plasmid-mediated Mcr-1, both of which confer resistance to polymyxins in certain Gram-negative bacteria via the addi-

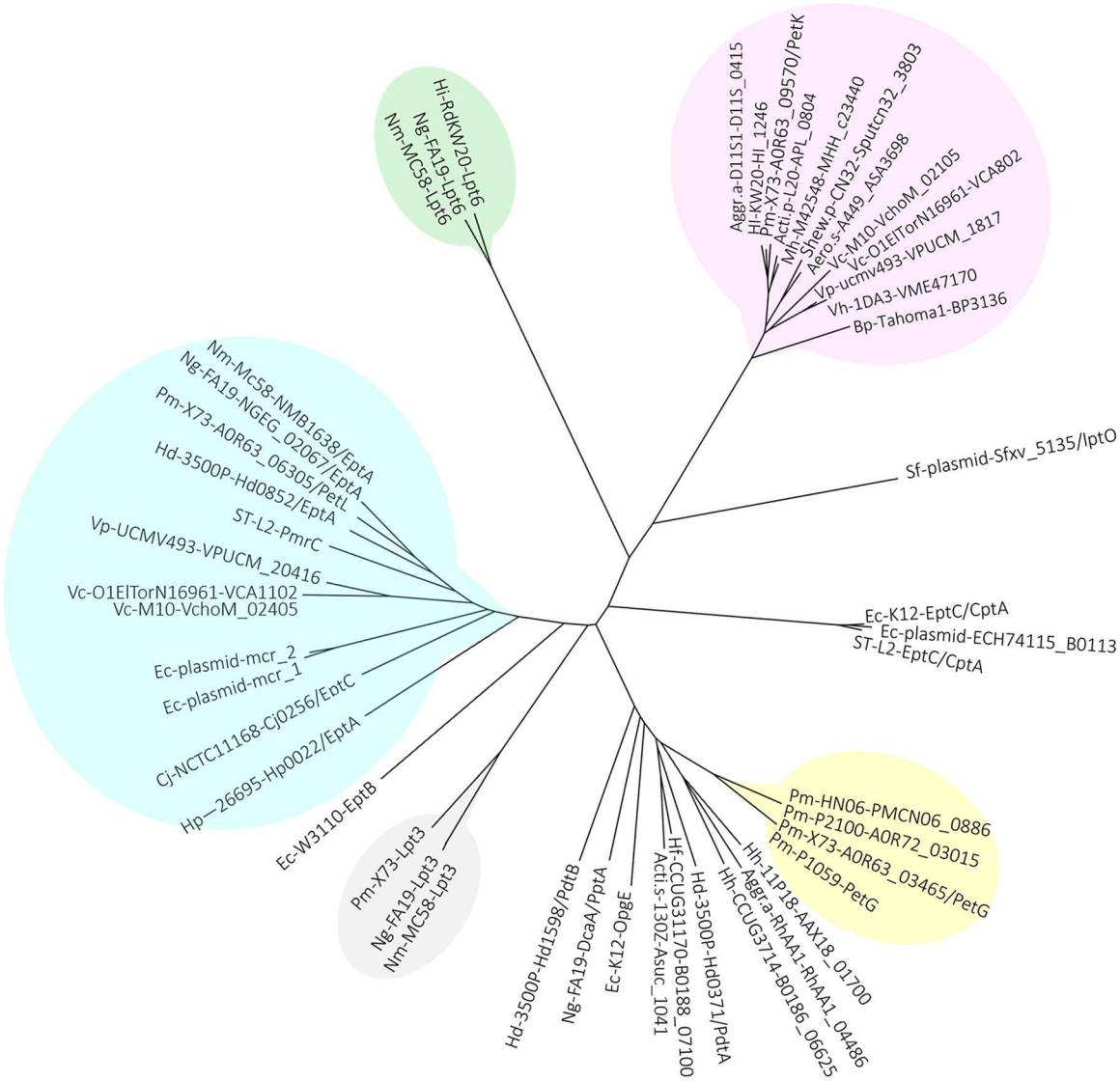

FIG 2 Phylogenetic analysis of a representative number of known and predicted phosphoethanolamine (PEtn) transferases. Shaded clusters represent five different PEtn transferase families as follows; blue, lipid A-specific PEtn transferases, including EptA; green, PEtn transferases specific for the 6 position of the second heptose (Hep II) in the inner core region of lipooligosaccharide/lipopolysaccharide (LOS/LPS); gray, PEtn transferases specific for the 3 position of Hep II in the inner core of LOS/LPS; yellow, PEtn transferases, including PetG (this study), specific for the addition of PEtn to galactose residues in LPS; pink, putative PEtn transferases predicted to transfer PEtn to 3-deoxy-D-manno-oct-2-ulosonic acid (Kdo), including the PEtn transferase PetP (this study). Labels indicate species, strain, and gene/locus tag, separated by hyphens. Bacterial species are indicated as follows; Acti.p, *Actinobacillus pleuropneumoniae*; Aero.s, *Aeromonas salmonicida*; Aggr.a, *Aggregatibacter actinomycetemcomitans*; Bp, *Bordetella pertussis*; Cj, *Campylobacter jejuni*; Ec, *Escherichia coli*; Hd, *Haemophilus ducreyi*; Hf, *Haemophilus felis*; Hh, *Haemophilus haemolyticus*; Hi, *Haemophilus influenzae*; Hp, *Helicobacter pylori*; Mh, *Mannheimia haemolytica*; Ng, *Neisseria gonorrhoeae*; Nm, *Neisseria meningitidis*; Pm, *Pasteurella multocida*; Sf, *Shigella flexneri*; Shew.p, *Shewanella putrefaciens*; ST, *Salmonella enterica* subsp. *enterica* serovar Typhimurium; Vc, *Vibrio cholerae*; Vh, *Vibrio harveyi*; Vp, *Vibrio parahaemolyticus*.

tion of PEtn to lipid A (16, 17), and *Campylobacter jejuni* protein EptC (18), a multifunctional transferase that can add PEtn to a range of cell components, including lipid A, heptose within the LPS inner core, and flagella (19–21). The amino acid sequences of these proteins, their active sites, and the associated metal binding sites are highly conserved. The presumed catalytic nucleophile in $EptA_{Nm}$ is Thr280, in EptC is Thr266, and in Mcr-1 is likely to be Thr285, as an *Escherichia coli* strain harboring a Mcr-1 with an Ala substitution at Thr285 lost resistance to polymyxin (15, 16, 18). The zinc coordination sites are Glu240/227/246, Asp452/427/465, and His 453/428/466 in $EptA_{Nm}$, EptC, and Mcr-1, respectively (15, 16, 18).

The multiple alignment data revealed that only four amino acids were conserved across all analyzed proteins. These were the Glu, Asp, and His residues (at 240, 452, and 453, respectively, in $EptA_{Nm}$) that form the zinc coordination site and a His at the position equivalent to 384 in $EptA_{Nm}$. (Fig. 2; see also Fig. S1). The presumed Thr catalytic residue (Thr 280 in $EptA_{Nm}$) was present in 34 of the 46 sequences. In the other 12 proteins, including *P. multocida* A0R63_09570, a serine residue was present at this position; these proteins formed a well-separated branch in the phylogenetic tree (Fig. 2, pink-shaded proteins).

The lipid A-specific PEtn transferases from a range of species formed a distinct branch on the phylogenetic tree and included the protein encoded by *P. multocida* X73 gene A0R63_06305 (Fig. 2, blue-shaded proteins). Accordingly, we predicted that the protein encoded by this gene would add PEtn to lipid A; thus, we named this gene *petL* (phosphoethanolamine onto lipid A). The transferases, which are specific for the addition of PEtn to Hep residues in the LPS inner core, formed three distinct branches (Fig. 2); the first contained Lpt-3 PEtn transferases specific for the addition of PEtn to the 3 position of Hep II, including the previously characterized proteins produced by *P. multocida* strain X73, *N. meningitidis*, and *N. gonorrhoeae*; the second contained Lpt-6 transferases from *N. meningitidis*, *N. gonorrhoeae*, and *H. influenzae* specific for the transfer of PEtn to the 6 position of Hep II; and the third contained CptA transferases from members of the *Enterobacteriaceae* family that are specific for the transfer of PEtn to Hep I.

P. multocida X73 protein A0R63_03465 grouped closely only with other *P. multocida* proteins from strains P1059, P2100, and HN06 (Fig. 2, yellow shading). This cluster was from a main branch that included two PEtn transferases with distinctly different acceptor molecules: glucose-specific OpgE from *E. coli* (which transfers PEtn to osmoregulated periplasmic glucans [OPG] [22]) and PptA from *N. gonorrhoeae* (strain FA1090) (which is responsible for the transfer of PEtn to pilin [23]). Also in this group were the predicted PEtn transferases PtdA and PtdB from *Haemophilus ducreyi*. The acceptor molecule targeted by these *H. ducreyi* PEtn transferases has not been identified, but these proteins were not required for the addition of PEtn to lipid A (24). There are no reports of PEtn decoration of cell components other than LPS in *P. multocida*, and this bacterium does not produce OPG. However, an alignment of the A0R63_03465 amino acid sequence with that of OpgE from *E. coli* revealed that they shared 31% amino acid identity (91% coverage), suggesting that X73 gene A0R63_03465 may encode a hexose-specific PEtn transferase. We therefore hypothesized that A0R63_03465 was a unique PEtn transferase required for the addition of PEtn onto the galactose residues at the distal end of the X73 LPS and named the gene *petG* (phosphoethanolamine onto galactose).

Importantly, the phylogenetic analysis revealed a well-separated and large group of proteins with unknown functions that included *P. multicoda* X73 protein A0R63_09570 (Fig. 2). A0R63_09570 shared amino acid identity with putative homologs (66% to 88% identity, 97% to 99% coverage) encoded on the genomes of a large number of other species belonging to the *Pasteurellaceae* family, including those within the genera *Actinobacillus*, *Aggregatibacter*, *Haemophilus*, and *Mannheimia.* More distant orthologs were also identified in species within the *Aeromonas*, *Bordetella*, *Shewanella*, and *Vibrio* genera (amino acid identity ranging from 50% to 55%, approximately 95% to 99% coverage). Surprisingly, a search of available protein structures revealed that a structure (resolved to 1.95 Å; PDB code 3LXQ) was available for the *Vibrio parahaemolyticus* protein within this group but the protein was identified only as a member of the alkaline phosphatase superfamily and no additional information was published. Previous analyses of the LPS produced by strains representing many of these genera revealed the presence of a single, usually phosphorylated Kdo molecule, with or without substitution with PEtn (3, 25–28). We therefore hypothesized that this cluster of proteins represented a new family of PEtn transferases that are specific for the addition of PEtn onto Kdo, and we named the X73 gene *petK* (phosphoethanolamine onto Kdo).

TABLE 1 Bacterial strains and plasmids used in this study

Strain or plasmid	Relevant description[a]	Source or reference
Strains		
E. coli DH5α	*deoR endA1 gyrA96 hsdR17*(r_k^- m_k^+) *recA1 relA1 supE44 thi-1* (*lacZYA-argFV169*) Φ80*lacZ* ΔM15 F^-	Bethesda Research Laboratories
E. coli SM10 λ pir	*E. coli* strain for propagation of pUA826 and its derivatives	30
P. multocida AL435	VP161 carrying a Tn*916* insertion in gene *pm1417*; fully virulent	29
P. multocida AL486	Single-crossover mutant of *petL* in AL435, constructed using pAL287	This study
P. multocida AL569	Single-crossover mutant of *petK* in AL435, constructed using pAL302	This study
P. multocida AL1354	*petL* TargeTron mutant of VP161, generated with pAL701	This study
P. multocida AL1405	*fis* TargeTron mutant of VP161	31
P. multocida AL1561	VP161 with expression vector pAL99	This study
P. multocida AL1563	VP161 with complementing plasmid pAL789 encoding *petG*	This study
P. multocida AL1911	*petG* TargeTron mutant of strain X73, generated with pAL910	This study
P. multocida AL2577	*petK* TargeTron mutant of VP161, generated with pAL1124	This study
P. multocida AL2581	AL1354 with complementing plasmid pAL1143 encoding *petL*	This study
P. multocida AL2583	AL1354 with expression vector pAL99	This study
P. multocida AL2601	AL2577 with vector pAL99S	This study
P. multocida AL2622	AL2577 with complementing plasmid pAL1151encoding *petK*	This study
P. multocida VP161	LPS genotype 1, capsule serogroup A, virulent poultry isolate	32
P. multocida X73	LPS genotype 1, capsule serogroup A, virulent poultry isolate	33
Plasmids		
pAL99	*P. multocida* expression plasmid (Kan^r)	8
pAL99S	*P. multocida* expression plasmid ($Spec^r$)	5
pAL287	Internal 1-kb fragment of VP161 *petL* cloned into pUA826 using primers BAP2569 and BAP2570	This study
pAL302	Internal fragment of VP161 *petK* cloned into pUA826 using primers BAP3425 and BAP3426	This study
pAL692	*P. multocida*-specific TargeTron vector, markerless intron (plasmid $Spec^r$)	31
pAL701	TargeTron vector pAL692 retargeted to *petL* in VP161 using primers BAP5870, BAP5871, and BAP5872 and EBS universal primer	This study
pAL789	Complete X73 *petG* gene cloned into expression plasmid pAL99 using primers BAP6116 and BAP6117	This study
pAL953	*P. multocida*-specific TargeTron vector (plasmid $Spec^r$, intron Kan^r)	5
pAL910	pAL692 TargeTron vector retargeted to *petG* in X73 using primers BAP6617, BAP6618, and BAP6619	This study
pAL1124	pAL953 TargeTron vector retargeted to *petK* in VP161 using primers BAP6715, BAP6716, and BAP6717	This study
pAL1143	Complete VP161 *petL* gene cloned into expression plasmid pAL99 using primers BAP7478 and BAP7479	This study
pAL1151	Complete *petK* gene cloned into expression plasmid pAL99S using primers BAP7509 and BAP7510	This study
pUA826	Mob^+, R6K replicon, single-crossover mutagenesis vector (Ap^r $Spec^r$)	34

[a]Ap^r, ampicillin resistance; $Spec^r$, spectinomycin resistance.

Construction of *P. multicoda* PEtn transferase mutants. In order to confirm the function of the predicted LPS PEtn transferases, directed mutants were generated in two fowl cholera isolates, VP161 and X73. Inactivation of *petL* and *petK* was achieved by single-crossover mutagenesis of strain AL435 (29), a tetracycline-resistant derivative of VP161 expressing wild-type LPS, to generate mutant strains AL486 and AL569, respectively (Table 1). In addition, *petL* and *petK* were inactivated in VP161 using Targetron mutagenesis to generate strains AL1354 and AL2577, respectively (Table 1). Finally, a *petG* mutant was generated using Targetron intron insertion into strain X73, as this gene is a pseudogene in VP161, generating mutant strain AL1911 (Table 1). All mutants showed normal *in vitro* growth rates equivalent to that of the wild type in heart infusion (HI) broth.

LPS analysis of *P. multocida* PEtn transferase mutants. Both of the *P. multicoda* wild-type strains, VP161 and X73, produced LPS glycoforms consistent with those previously published (3, 10). Similarly, parent strain AL435, used in the construction of single-crossover mutants, produced all of the LPS glycoforms observed in wild-type VP161 (Table 2), including two glycoforms previously determined to contain different lipid A-OH species (952 and 1,075 amu) (3), with the smaller of the two corresponding to lipid A-OH without PEtn and the larger corresponding to lipid A-OH with PEtn. Examination of the LPS produced by *petL* mutant AL486, generated by single-crossover

TABLE 2 Negative-ion CE-ES-MS data and proposed compositions of O-deacylated LPS and core oligosaccharide for *P. multocida* strains[a]

Strain	Observed ion (*m/z*)			Molecular mass (Da)		Proposed composition[b]
	$(M-4H)^{4-}$	$(M-3H)^{3-}$	$(M-2H)^{2-}$	Observed	Calculated	
Control strains						
VP161* wild-type strain	744.0	992.4		2,980.1	2,978.8	2PCho, 3Hex, 4Hep, 2Kdo, lipid A-OH
	749.0	999.6		3,000.9	3,000.8	2PCho, 4Hex, 4Hep, Kdo-P, lipid A-OH
	774.0	1,033.0		3,101.0	3,101.9	2PCho, 3Hex, 4Hep, 2Kdo, lipid A-OH-PEtn
	780.0	1,040.0		3,123.5	3,123.8	2PCho, 4Hex, 4Hep, Kdo-P, PEtn, lipid A-OH
	780.0	1,040.0		3,123.5	3,123.8	2PCho, 4Hex, 4Hep, Kdo-P, lipid A-OH-PEtn
	810.0	1,081.0		3,245.0	3,246.9	2PCho, 4Hex, 4Hep, Kdo-P-PEtn, lipid A-OH-PEtn
X73* wild-type strain		1,033.8		3,104.4	3,101.9	2PCho, 3Hex, 4Hep, 2Kdo, PEtn, lipid A-OH
		1,040.1		3,123.3	3,123.8	2PCho, 4Hex, 4Hep, Kdo-P, PEtn, lipid A-OH
		1,073.1		3,222.3	3,224.9	2PCho, 3Hex, 4Hep, 2Kdo, 2PEtn, lipid A-OH
	810.9	1,081.5		3,247.6	3,246.9	2PCho, 4Hex, 4Hep, Kdo-P, 2PEtn, lipid A-OH
		1,116.2		3,351.6	3,348.0	2PCho, 3Hex, 4Hep, 2Kdo, 2PEtn, lipid A-OH-PEtn
	841.6	1,122.4		3,370.3	3,369.9	2PCho, 4Hex, 4Hep, Kdo-P, 3PEtn, lipid A-OH
	872.5	1,163.5		3,493.8	3,493.0	2PCho, 4Hex, 4Hep, Kdo-P, 3PEtn, lipid A-OH-PEtn
VP161 Tet^{r}[d]	743.7	991.8	1,488.5	2,978.7	2,978.8	2PCho, 3Hex, 4Hep, 2Kdo, lipid A-OH
(AL435)	749.3	999.4	1,499.1	3,000.9	3,000.8	2PCho, 4Hex, 4Hep, Kdo-P, lipid A-OH
	780.0	1,040.2	1,560.8	3,123.7	3,123.8	2PCho, 4Hex, 4Hep, Kdo-P-PEtn, lipid A-OH
PetG study						
X73 *petG* intron mutant		1,040.1		3,123.3	3,123.8	2PCho, 4Hex, 4Hep, Kdo-P, PEtn, lipid A-OH
(AL1911)		1,081.0		3,246.0	3,246.9	2PCho, 4Hex, 4Hep, Kdo-P, PEtn, lipid A-OH-PEtn
VP161 + plasmid encoded *petG*	811.0	1,081.5		3,247.8	3,246.9	2PCho, 4Hex, 4Hep, Kdo-P, PEtn, lipid A-OH-PEtn
(AL1563)	841.5	1,122.0		3,369.5	3,369.9	2PCho, 4Hex, 4Hep, Kdo-P, 2PEtn, lipid A-OH-PEtn
	872.0	1,163.0		3,492.0	3,493.0	2PCho, 4Hex, 4Hep, Kdo-P, 3PEtn, lipid A-OH-PEtn
PetL study						
petL mutant[c] in VP161	743.8	991.9	1,488.6	2,979.0	2,978.8	2PCho, 3Hex, 4Hep, 2Kdo, lipid A-OH
(AL486)	749.3	999.4	1,499.3	3,001.0	3,000.8	2PCho, 4Hex, 4Hep, Kdo-P, lipid A-OH
	780.0	1,040.2	1,560.0	3,123.2	3,123.8	2PCho, 4Hex, 4Hep, Kdo-P-PEtn, lipid A-OH
petL intron mutant in VP161	743.5	991.5		2,977.8	2,978.8	2PCho, 4Hex, 4Hep, 2Kdo, lipid A-OH
(AL1354)	749.0	999.0		3,000.0	3,000.8	2PCho, 4Hex, 4Hep, Kdo-P, lipid A-OH
	780.0	1,040.0		3,123.5	3,123.8	2PCho, 4Hex, 4Hep, Kdo-P-PEtn, lipid A-OH
PetK study						
petK mutant[c] in VP161	743.8	992.2	1,488.5	2,979.3	2,978.8	2PCho, 3Hex, 4Hep, 2Kdo, lipid A-OH
(AL569)	749.3	999.3	1,499.5	3,001.0	3,000.8	2PCho, 4Hex, 4Hep, Kdo-P, lipid A-OH

[a]CE-ES-MS, capillary electrophoresis coupled to electrospray-mass spectrometry.
[b]Proposed compositions and locations of PEtn residues are based on the full structural analysis of VP161 and X73 LPS (35). Average mass units were used for the calculation of molecular masses based on the following proposed composition: lipid A, 953.01; Hex, 162.14; Hep, 192.17; Kdo, 220.18; Kdo-P, 300.16; PEtn, 123.05; PCho, 165.18.
[c]Mutant generated by single-crossover mutagenesis in VP161 tetracycline-resistant strain AL435.
[d]Tetracycline-resistant (Tet^{r}) strain AL435 was used to generate single-crossover mutants via conjugation.

mutagenesis in strain AL435, revealed the loss of all charged ions representing the LPS glycoforms corresponding to the larger lipid A-OH species with PEtn. To confirm the result, the *petL* TargeTron mutant (AL1354; Table 1) was also examined. LPS analysis of this second mutant also revealed charged ions corresponding to LPS glycoforms that contained only the smaller lipid A species (Table 2) (3). Together, these data confirm that *petL* encodes the PEtn transferase required for the addition of PEtn to lipid A in *P. multocida*.

Previous structural data revealed that the LPS produced by X73 contains a PEtn residue on the 6 position of both galactose residues located at the distal end of the LPS molecule (10). The LPS structure produced by VP161 is identical to the X73 structure except that the LPS structure does not have the PEtn residues (3). Consistent with this finding was the fact that the predicted galactose-specific PEtn transferase *petG* gene was intact in strain X73 but was present as a pseudogene in VP161. To prove that PetG was the PEtn transferase responsible for the addition of PEtn to each of the terminal galactose residues on the X73 LPS, we examined the LPS produced by X73 *petG* TargeTron mutant AL1911 (Table 1). LPS structural analysis of AL1911 revealed that the LPS glycoform profile was highly similar to the profile from strain VP161, with the

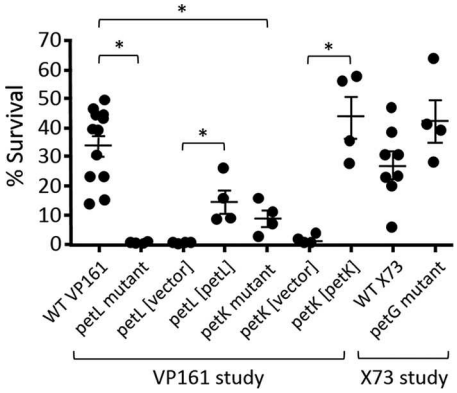

FIG 3 Sensitivity of *P. multocida* to the chicken antimicrobial peptide cathelicidin-2. Percentages of survival were determined by dividing the CFU count per milliliter following incubation in 2.5 μM cathelicidin-2 at 37°C for 3 h by the CFU count per milliliter following incubation in vehicle only. Each data point shows the percent survival of each strain in the presence of cathelicidin-2 for a single assay. The average percent survival is indicated by the horizontal bars $\pm$ standard error of the mean. For the VP161 study, the differences between the mean levels of survival of the parent and mutant (*petL* or *petP*) were significant, as were the differences between the data determined for the mutant (*petL* or *petP*) provided with vector and the data determined for the complemented mutant. In contrast, inactivation of *petG* had no effect on the ability of strain X73 to resist the action of cathelicidin-2. *, $P < 0.05$.

number of PEtn residues detected in the oligosaccharide (LPS-OH) sample consistently lower than in the LPS-OH sample from the wild-type parent X73 strain (Table 2). Given that the only sugars in the oligosaccharide component of genotype 1 LPS known to be decorated with PEtn are the terminal galactose residues (10), we concluded that *petG* is the galactose-specific PEtn transferase. To provide further evidence, we provided strain VP161 with pAL789, containing the functional *petG* from X73 on expression plasmid pAL99, generating strain AL1563 (Table 1). Heterologous expression of X73 PetG in VP161 resulted in a strain producing LPS glycoforms containing additional PEtn residues relative to LPS glycoforms produced by VP161 and VP161 containing empty pAL99 (AL1561) (Table 2). Importantly, structural analysis of the LPS produced by VP161 containing a functional copy of *petG* (AL1563) identified new triply charged ions at *m/z* 1,122 and 1,163 consistent with one and two additional PEtn residues present in the AL1563 LPS core oligosaccharide component (Table 2).

To prove our hypothesis that PetK was the transferase required for the addition of PEtn to the phosphate on the Kdo residue, we examined the LPS produced by *petK* mutant AL569 (Table 1). LPS structural analysis of AL569 revealed the absence of the doubly, triply, and quadruply charged ions at *m/z* 1,560, 1,040, and 780, which correspond to an O-deacylated molecule containing one PEtn residue in parent strain AL435 (Table 2). Tandem MS (MS/MS) analysis of AL435 had established that this single PEtn residue was not located on the O-deacylated lipid A molecule (data not shown). Based on previous structural analysis of LPS produced by VP161 and AL435 (36), the absence of these ions in the spectra must correspond to the absence of PEtn on Kdo-P in LPS glycoform A. Thus, these data show that VP161 *petK* mutant AL569 did not produce any LPS glycoforms containing a PEtn molecule on phosphorylated Kdo. Therefore, these data are consistent with PetK being the PEtn transferase specific for the addition of PEtn to Kdo-P in *P. multocida*.

Susceptibility of the *P. multocida* X73 and VP161 PEtn transferase mutants to cathelicidin-2. The susceptibility of each of *P. multocida petL*, *petK*, and *petG* Targetron mutants AL1354, AL2577, and AL1911, respectively (Table 1) to chicken antimicrobial peptide cathelicidin-2 was assessed alongside each of the wild-type parent strains, VP161 and X73 (Fig. 3). After 3 h of incubation in the presence of 2.5 μM cathelicidin-2, the two wild-type parent strains, VP161 and X73, had survival rates of 34% and 27%, respectively, relative to the growth of each strain in the absence of cathelicidin-2. The X73 *petG* mutant (AL1911) did not display increased susceptibility to cathelicidin-2. In

TABLE 3 Virulence of the *P. multocida* VP161 *petK* and *petL* phosphoethanolamine transferase mutant strains, as determined by direct challenge in chickens

Route of challenge	Strain	Dose (CFU)	No. of deaths/total no. of chickens[a]	Avg time to death (h)
Intramuscular	Wild-type *P. multocida* VP161	1.9×10^3	10/10	18.7 ± 2.3
	VP161 *petL* mutant	1.4×10^3	10/10	17.9 ± 1.8
	VP161 *petK* mutant	1.3×10^3	10/10	18.2 ± 3.2
Intratracheal	Wild-type *P. multocida* VP161	1.9×10^7	10/10	18.7 ± 5.0
	VP161 *petL* mutant	1.4×10^7	10/10	15.4 ± 3.0
	VP161 *petK* mutant	1.3×10^7	10/10	14.8 ± 3.4

[a]All birds showing terminal signs of fowl cholera were euthanized in accordance with animal ethic requirements.

contrast, the survival rates of the VP161 *petL* mutant (AL1354) and the VP161 *petK* mutant (AL2577) were dramatically reduced to 0.3% and 9%, respectively, relative to growth of the same strain in the absence of cathelicidin-2 (Fig. 3). Complementation of the VP161 *petL* mutant with an intact copy of *petL* on expression vector pAL99 (AL2581) partially restored the survival rate in the presence of cathelicidin-2 (14.6%). Complementation of the *petK* mutant with an intact copy of *petK* on expression vector pAL99 (AL2622) fully restored survival rates in the presence of cathelicidin-2 to wild-type levels (44%). In contrast, the *petL* and *petK* VP161 mutants containing the pAL99 vector only (AL2583 and AL2601, respectively) remained susceptible to the action of cathelicidin-2 (0.4% and 1.3%, respectively) (Fig. 3). The increased sensitivity of *P. multocida* following inactivation of either *petL* or *petK* was confirmed with cathelicidin-2 assays using the VP161 *petL* and *petK* mutants (AL486 and AL569, respectively; Table 1) that were generated using single-crossover mutagenesis (data not shown). Together, these data show that the addition of PEtn to lipid A by PetL, and the addition of PEtn to Kdo-P by PetK, is critical for strain VP161 to resist the action of cathelicidin-2.

Virulence of the *petK* and *petL* VP161 mutants. The *petK* and *petL* VP161 Targetron mutants that showed increased susceptibility to the antimicrobial cathelicidin-2 (AL2577 and AL1354, respectively) were assessed for their ability to cause disease in the natural chicken host. *P. multocida* wild-type parent strain VP161, the *petK* mutant (AL2577), and the *petL* mutant (AL1354) were separately used to challenge two groups of 10 birds. The first group of birds received the designated *P. multocida* strain intramuscularly (i.m.) via injection into the pectoral muscle of each bird, while the second group received the strain via intratracheal (i.t.) inoculation, which mimics the natural route of infection. All birds that were challenged i.m. with parent strain VP161 showed late-stage signs of disease within 24 h and were euthanized (Table 3). Similarly, all birds injected i.m. with either the VP161 *petK* mutant or the VP161 *petL* mutant showed late-stage signs of disease at times similar to those seen with birds infected with the wild-type strain and were euthanized (Table 3). Moreover, birds that were challenged via the intratracheal route with parent strain VP161, *petK* mutant AL2577, or *petL* mutant AL1354 succumbed to disease within a similar time frame (Table 3). Muscle (i.m. groups only) and liver samples were recovered from a representative number of birds within each group immediately following euthanasia, and the samples were plated onto nonselective HI medium. All colonies that grew on the plates had typical *P. multocida* morphology, and PCR analysis of a representative sample of the recovered colonies revealed that the strain used to challenge each group was present in the corresponding samples. Together, these data demonstrate that the *petK* and *petL* VP161 mutants were capable of causing systemic disease in chickens. Thus, addition of PEtn to lipid A in glycoform A and B or to Kdo-P in glycoform A LPS is not required for *P. multocida* to cause fowl cholera disease in the natural host.

PEtn gene expression in VP161 and VP161 regulatory mutants. To identify if any of the PEtn genes were differentially expressed during growth of VP161 in the early exponential, mid-exponential, and late exponential growth phases, available transcriptomic data for each gene were examined. Also included in the analysis were transcrip-

TABLE 4 Relative expression levels of PEtn transferase genes *petL*, *petK*, *lpt3*, and *petG* and of regulatory genes *hfq* and *fis* in wild-type strain VP161 during the late exponential-growth phase (relative to expression during the early exponential-growth phase) and expression in the VP161 *fis* and *hfq* mutants relative to expression in WT strain VP161 in the same growth phase[a]

	Expression in WT during late exponential growth compared with early exponential-growth phase			Expression in *fis* mutant relative to expression in WT during early exponential-growth phase			Expression in *hfq* mutant relative to expression in WT during mid-exponential-growth phase[c]		
Gene	Expression ratio (log_2)	Fold change	FDR	Expression ratio (log_2)	Fold change	FDR	Expression ratio (log_2)	Fold change	FDR
fis	−2.84	7.1 ↓	2.5e−6	−0.84	NS	0.01	0.86	NS	0.03
hfq	−0.43	NS	0.05	−1.13	2.2 ↓	9.7e−4	−0.56	NS	0.07
petL	−5.67	50.9 ↓	4.5e−7	−5.58	47.8 ↓	9.4e−7	1.94	3.8 ↑	1.3e−3
petK	−0.12	NS	0.60	−0.84	NS	8.0e−3	−0.12	NS	0.63
lpt3[b]	2.13	4.4 ↑	2.3e−4	−0.44	NS	0.43	−0.32	NS	0.56
petG[b]	1.18	2.3 ↑	4.7e−3	0.06	NS	0.90	0.14	NS	0.73

[a]Genes were identified as differentially expressed if they displayed a change in expression across the duplicate samples of ≥1.0 log_2 (≥2.0-fold) at a false-discovery rate (FDR) of ≤0.05. NS, no significant change; WT, wild type.
[b]Pseudogenes in VP161 due to single-point mutation but with both genes intact in strain X73.
[c]Data are from Mégroz et al. (37).

tomic data obtained from a VP161 strain with an inactivating mutation in *fis* (unpublished data), encoding the growth-phase-dependent transcriptional regulator Fis and data from a VP161 *hfq* mutant unable to produce Hfq, a protein essential for the activity of many small RNA (sRNA) regulatory molecules (37). The expression values for the four LPS PEtn genes, *petL*, *petK*, *lpt3*, and *petG*, and for the two regulatory genes *fis* and *hfq* during early exponential growth of the wild-type strain VP161 were compared to the expression values determined during late-exponential growth (Table 4). The expression levels of *hfq* and *petK* were unchanged in the wild-type VP161 strain during these two growth phases. However, expression of *petL*, encoding the lipid A-specific PEtn transferase, was reduced more than 50-fold (log_2 ratio, −5.67; false-discovery rate [FDR], 4.5×10^{-7}) during late exponential growth compared to early exponential growth. The *fis* gene also showed a 7.1-fold reduction in expression during late exponential growth (log_2 ratio, −2.84; FDR, 2.5×10^{-6}; Table 4), confirming its growth-phase-dependent expression reported previously for *P. multocida* (31) and other organisms. In contrast, transcript levels from *lpt3* and *petG* (both intact in X73 but both present as pseudogenes in VP161 due to single point mutations) showed significant 4.4-fold and 2.3-fold increases (FDR = 2.3×10^{-4} and FDR = 4.7×10^{-3}, respectively; Table 4) at the late exponential growth phase. The expression of the same set of genes was then analyzed in the VP161 *fis* mutant (compared with expression in the wild-type strain) during the early exponential growth phase, when Fis is most active (31). There was no change in expression of *petK*, *lpt3*, or *petG* in the *fis* mutant. However, there was a major reduction in expression of *petL* in the *fis* mutant compared to expression in VP161 (−47.8-fold; FDR, 9.4×10^{-7}). Thus, expression of *petL* is dependent on the presence of Fis. In addition, as reported previously (37), *fis* inactivation in VP161 also resulted in reduced expression of *hfq* (2.2-fold reduction; log_2 ratio, −1.13; FDR, 9.7×10^{-4}). A similar comparison was performed using the gene expression values obtained from the published transcriptomic study on the VP161 *hfq* mutant (31) (Table 4). There was no change in expression of *fis* following inactivation of *hfq* in VP161, nor was there any change in expression of the PEtn genes, except for *petL*, whose expression increased 3.8-fold in the *hfq* mutant (log_2 ratio, 1.94; FDR, 1.3×10^{-3}). Together, these data show that expression of *lpt3* and *petG* is greatest during late exponential growth but that *petL* expression is greatest during early exponential growth, when Fis is at its most active. Together with the *fis* and *hfq* mutant transcriptomic data, these data indicate that *petL* is positively regulated by Fis and negatively regulated by a Hfq-dependent sRNA molecule.

DISCUSSION

PEtn is a phosphomonoester that is used by eukaryotic cells during membrane biosynthesis and by bacteria for the decoration of multiple surface structures, including

LPS, flagella, and type IV pili (20, 38, 39). PEtn is also incorporated into OPG, located in the periplasm of many bacteria, including *E. coli* (22). The addition of PEtn to key positions on bacterial surface structures confers resistance to polymyxins and host innate immune antimicrobials, including cathelicidins and alpha and beta defensins (21, 24, 40). The most common surface structure to be decorated with PEtn in Gram-negative bacteria is the LPS structure, where it can be attached to lipid A, to Kdo, to Hep within the inner core, or to the outer core galactose (10, 38, 41–43).

At least six PEtn transferase types, each required for the attachment of PEtn to specific residues on LPS, have been identified and characterized in other Gram-negative bacteria. The best-characterized LPS PEtn transferase is EptA, which adds PEtn to the 1 or 4′ position of lipid A in *N. meningitidis* (11) and in many other bacteria. EptB is a PEtn transferase produced by *E. coli* that adds PEtn to the 7 position of the outer Kdo residue on LPS (44), and LptO is a plasmid-encoded transferase that adds PEtn to rhamnose in the O-antigen produced by *Shigella flexneri* (45). Finally, the heptose-specific transferases, Lpt-3 and Lpt-6, transfer PEtn to the 3 position and 6 position of Hep II, respectively, in the LPS produced by *P. multocida* (Lpt-3 only), *Neisseria* spp., and *Haemophilus* spp. (12–14) and EptC/CptA adds PEtn to Hep I in the LPS produced by *E. coli* (46) and many other species belonging to the *Enterobacteriaceae* family.

In this study, we characterized the function of three LPS-associated PEtn transferases produced by *P. multocida* using a combination of bioinformatics, directed mutagenesis, and LPS structural analyses. Furthermore, we have shown that two of the PEtn transferases, PetL and PetK, are critical for mediating the resistance of *P. multocida* fowl cholera strain VP161 to the chicken antimicrobial peptide cathelicidin-2. *P. multocida* PEtn transferase PetL is an EptA homologue and is responsible for the addition of PEtn to the 4′ position on lipid A. We predict that PEtn addition to lipid A will also be critical for conferring resistance to other antimicrobial agents whose action relies on a charged interaction with lipid A. In *N. gonorrhoeae*, the PEtn on lipid A mediates resistance to the classical complement pathway, is important for bacterial attachment to host cells, and also modulates the host immune response (40). Our direct virulence study indicates that the *P. multocida petL* mutant was still able to cause systemic disease when delivered intramuscularly or via the trachea. Moreover, inactivation of *petL* in VP161 had no effect on serum resistance (data not shown). Whether the loss of PEtn from *P. multocida* lipid A affects the binding of the bacterium to host cells or interaction with other components of the immune system will be the subject of future studies.

Importantly, we report for the first time the identification of two PEtn transferases with novel acceptor molecules. Phylogenetic analysis revealed that PetK represents the first member of a new family of PEtn transferases (Fig. 2). LPS structural analysis of the *petK* mutant, AL569, demonstrated that PetK is responsible for the addition of PEtn to the single, phosphorylated Kdo molecule on the glycoform A LPS in *P. multocida*. The addition of PEtn to this key position on the LPS molecule is also important for *P. multocida* strain VP161 resistance to the action of cathelicidin-2, although the *petK* mutant retained wild-type levels of virulence in chickens. The addition of PEtn to a single, phosphorylated Kdo molecule has been reported for other Gram-negative bacteria, including *H. influenzae* (substituting the phosphate group at the 4 position of the Kdo molecule) and *Vibrio cholerae* (27, 47). A search of numerous genomes representing *H. influenzae* strains revealed only one gene in each with significant identity to PetK at the amino acid level. For example, the product of the gene at locus tag HI_1246 in *H. influenzae* strain KW20 shares 76% identity with PetK. We suggest that this gene and homologs in other strains encode the PEtn transferase required for the addition of PEtn onto Kdo in those species that produce LPS containing a single Kdo residue. Strains belonging to the *Vibrio* genus also produce LPS with only one Kdo residue. Analysis of the LPS produced by *V. cholerae* serogroup O139 strain MO10-T4 showed that PEtn was on the 7 position of the single Kdo molecule whereas phosphate was retained at the 4 position (47). Although the genome sequence was not available for MO10-T4, the acapsular mutant strain used in the LPS study cited above, an analysis of the parent strain genome (MO10) revealed only one encoded protein (locus tag

VchoM_02105) that shared significant identity (53% identity, 97% coverage) with PetK; this protein also clustered within the same branch of the phylogenetic tree as PetK (Fig. 2). Many other *Vibrio* strains also encode a protein that shares significant identity with PetK (e.g., VCA0802 in O1 biovar El Tor strain N16961: 58% identity, 100% coverage). Interestingly, a search of the publicly available protein structures revealed that the structure of one protein within the PetK PEtn transferase family has been determined. This alkaline phosphatase family protein (PDB code 3LXQ) from *V. parahaemolyticus* (strain not stated) has homologs in many strains belonging to the species and is of unknown function. The amino acid sequence of the crystalized protein is a 100% match to a sequence in the central region of a predicted protein within a number of *V. parahaemolyticus* strains, including VPUCM_ 1871 in strain UCMV493 (Fig. 2). It is possible, given that the protein clusters within the same branch as PetK, that VPUCM_ 1871 represents the PEtn transferase required for the addition of PEtn to Kdo in *Vibrio* spp.

The second novel PEtn transferase identified in this work was PetG from *P. multocida* strain X73. Inactivation of *petG* and subsequent LPS structural studies showed that *petG* was required for the unusual addition of PEtn to the 6 position on the Gal residues in the X73 LPS outer core. These Gal residues are also decorated with PCho at the 3 position (10), and this addition has been shown to be essential in strain VP161 for wild-type levels of resistance to cathelicidin-2 and for growth of VP161 *in vivo* in chickens (36). However, PEtn substitution of these Gal residues in the X73 LPS is not required for virulence, as mutation of *petG* in X73 did not affect virulence in chickens (data not shown). PEtn on Gal is also unlikely to play a role in resistance to cathelicidin antimicrobials as mutation of *petG* had no effect on the ability of strain X73 to resist the action of cathelicidin-2 (Fig. 3). Phylogenetic analysis showed that PetG clustered closely only with putative transferases from other *P. multocida* strains. However, its closest relatives outside the *Pasteurella* genus were PptA from *N. gonorrhoeae*, which adds PEtn to Ser within the type IV pilus major subunit; PilE (48); and OpgE from *E. coli*, which transfers PEtn to glucose in OPG.

The addition of PEtn to *P. multocida* LPS is nonstoichiometric in all strains examined to date. This may be due to the regulated expression of the PEtn transferase genes, availability of the enzyme acceptor molecules, and/or the activity of each PEtn transferase. Some *P. multocida* strains belonging to LPS genotype L1 express LPS glycoforms similar to those expressed by VP161, with a complete absence of PEtn on the inner core Hep II and the terminal Gal residues (4). We predict that these strains, like VP161, also have inactivating mutations in *lpt3* and *petG*. The presence or absence of PEtn on Hep II on the LPS is important for the serological differentiation of *P. multocida* strains belonging to LPS genotype 2 (13). In *N. meningitis*, Lpt-3 is important both for immunological recognition and for resistance to antimicrobial agents and expression of *lpt3* is controlled by the two-component signal transduction system (TCSTS) MisR/MisS (49). There have been no reported studies on *P. multocida* TCSTS, but the genomes of strains X73 and VP161, which are very similar, each contain six predicted TCSTS as well as two genes encoding putative hybrid response regulator/sensor kinase proteins. It is likely that one or more regulators are involved in the regulation of expression of some of the *P. multocida* PEtn transferases. Whole-genome RNA expression analyses of *P. multocida* strain X73 revealed a significant increase in *lpt3* expression during the late stages of *P. multocida* infection in chickens compared to growth *in vitro* (50), corresponding to the observation that PEtn is not present on Hep II in LPS isolated from X73 grown *in vitro* (10). In contrast, expression of *petL* was significantly decreased during late-stage *in vivo* growth (*petL in vivo* expression was reduced between 1.7-fold and 3.8-fold in bacteria isolated from blood and between 2.7-fold and 5.1-fold in bacteria isolated from liver), indicating that addition of PEtn to lipid A is reduced during late stages of systemic infection (our unpublished data). These data suggest that there is regulatory control of *lpt3* and *petL* expression and that PEtn addition to Hep II and Kdo-P may not occur at the same time. Transcriptomic analyses of *in vitro*-grown *P. multocida* strain VP161 comparing gene expression during the early log phase with that seen during late log-phase growth also indicated an inverse relationship between the

levels of expression of *petL* and *lpt3* (Table 4). Expression of *petL* was 50.9-fold higher in early exponential-phase cultures than in late exponential-phase cultures, whereas levels of transcripts from *petG* and *lpt3* were greatest during late-exponential-phase growth (2.3-fold and 4.4-fold increases compared to early log expression, respectively) (Table 4). Moreover, growth-phase-dependent changes in *petL* expression correlate strongly with the abundance of the global regulatory protein Fis, expression of which is greatest during early log-phase growth (7.2-fold higher in early log phase compared to late log phase). Transcriptomic analyses from two *P. multocida* VP161 regulatory mutants revealed that *petL* expression was dramatically (48-fold) decreased following *fis* inactivation but increased when *hfq* was inactivated (37), suggesting that Fis and Hfq are involved in the control of PEtn decoration of the *P. multocida* lipid A molecule. Together, the data indicate that the relative positions of the PEtn residues on the *P. multocida* LPS molecule may change during different growth phases. A study of human and mouse urinary tract infections has shown that cathelicidins are produced very early in infection due to a rapid response from epithelial cells, followed shortly by the infiltration of cathelicidin-producing leukocytes (51). We have shown that *petL*, which adds PEtn to lipid A, is expressed most highly early in the growth of *P. multocida* and that its action provides protection against cathelicidin-2. Conversely, we have shown that expression of *lpt3* is low early in infection and high late in infection. Thus, it is possible that the regulated addition of PEtn at different positions on the LPS may play important roles at some stage of *P. multocida* pathogenesis. Future studies will be focused on mapping the regulatory network that controls the expression of these important LPS PEtn transferase genes.

MATERIALS AND METHODS

Bacterial strains, plasmids, media, and growth conditions. The bacterial strains and plasmids used in this study are listed in Table 1. *E. coli* and *P. multocida* were grown routinely in lysogeny broth (LB) and heart infusion (HI) broth, respectively (Oxoid, Australia), supplemented with kanamycin (Kan; 50 μg/ml), or spectinomycin (Spec; 50 μg/ml) when required. Solid media were obtained by the addition of 1.5% (wt/vol) agar. Isolation of LPS from *P. multocida* was performed as described previously (5).

Bioinformatic analyses. Putative PEtn transferase genes were identified by searching the available genomes at the National Center for Biotechnology Information (NCBI) and Pathosystems Resource Integration Center (PATRIC) using one or more of the following bioinformatics tools: the protein-protein basic local alignment search tool (BLASTP), the conserved domain database (CDD), and the transmembrane helices hidden Markov model (TMHMM). Multiple-sequence alignments were performed using the constraint-based multiple alignment tool COBALT available at NCBI. For phylogenetic analysis, the alignment data (output newick) were visualized with FigTree 1.4.3, developed by the Molecular Evolution, Phylogenetics and Epidemiology Group at Biological Sciences, University of Edinburgh (http://tree.bio.ed.ac.uk/). The Vector Alignment Search Tool (VAST), available through NCBI, was used to identify proteins with structural similarity.

DNA manipulations. Restriction digests and ligations were performed using enzymes and buffers obtained from NEB or Roche Diagnostics GmbH. Plasmid DNA and genomic DNA were prepared using a plasmid minikit (Qiagen) and a genomic DNA extraction kit (RBC), respectively. PCR amplification of DNA was performed using *Taq* DNA polymerase or an Expand High Fidelity PCR system (Roche Diagnostics), and amplified fragments were purified using a Qiagen PCR purification kit. The oligonucleotides used in this study were synthesized by Sigma (Australia) and are listed in Table S1 in the supplemental material. Transformation of *P. multocida* via electroporation was performed as described previously (31). DNA sequencing reactions were performed with BigDye Terminator version 3.1 (Applied Biosystems) using plasmid DNA. The use of PCR products or genomic DNA as the template and the amplification conditions were described previously (5, 52). All DNA sequences were determined on a capillary-platform genetic analyzer (Applied Biosystems 3730) and analyzed with Vector NTI Advance 11 (Invitrogen).

Construction of *P. multocida* mutants. Plasmids used for the mutagenesis of *P. multocida* genes are listed in Table 1. The inactivation of genes in *P. multocida* strain VP161 using single-crossover mutagenesis (strains AL569 and AL486) was performed as described previously (29). For the generation of the *petL* and *petK* single-crossover mutants (AL486 and AL569), conjugation was performed using a donor *E. coli* strain containing a gene-specific pUA826-derived plasmid together with a tetracycline-resistant *P. multocida* strain, AL435, as the recipient to allow for counterselection following conjugation. Transconjugants were selected on solid agar with the appropriate antibiotic selection. Transconjugants with an insertion of a pUA826-derived plasmid were identified by PCR screening using primers flanking the target gene in combination with an outward firing, pUA826-specific primer located within the integrated plasmid (29). For the generation of group II intron insertional mutants in *P. multocida* strains VP161 and X73, we used the TargeTron mutagenesis method (Sigma-Aldrich) as described previously (5, 31) with oligonucleotides designed using the TargeTron design site (Sigma-Aldrich) (Table S1). Plasmids contain-

ing a group II intron retargeted to the target gene (Table 1) were used to transform *P. multocida* wild-type strains VP161 and X73 via electroporation. For the identification of intron mutants, transformants were screened for the correct intron insertion in the *P. multocida* genome as described previously (5). The presence of a single intron located in the target gene was determined using direct sequencing from genomic DNA as described previously (5) and the intron-specific EBS universal primer (Table S1).

In *trans* complementation of mutants. For complementation experiments, expression plasmid pAL99 (kanamycin resistant [Kan^r]) or expression plasmid pAL99S (spectinomycin resistant [Spec^r]) was used as described previously (5). In brief, a complete copy of the PEtn transferase gene was amplified from the parent strain using an appropriately designed pair of oligonucleotide primers (Table S1). The PCR product was column purified and then ligated to the expression vector using BamHI and SalI restriction sites as described previously (5). The ligated products were then used to transform electrocompetent *P. multocida* cells. Putative recombinant plasmids in the transformants were analyzed by colony PCR followed by DNA sequencing, as described previously (5).

Lipopolysaccharide compositional analyses. O-deacylated LPS (LPS-OH), core oligosaccharide (OS), and completely deacylated LPS were all isolated and purified from LPS as described previously (3). To identify the locations of PEtn substitutions, ^{31}P-^{1}H-labeled heteronuclear single quantum coherence (HSQC) experiments were performed (3).

Antimicrobial peptide sensitivity assays. The MIC of the chicken antimicrobial peptide cathelicidin-2 (RVKRVWPLVIRTVIAGYNLYAIKKK; a gift from H. Haagsman, Utrecht University) against *P. multocida* strains was determined using a modified antimicrobial peptide microdilution assay as described previously (35). Briefly, cell suspensions for each *P. multocida* strain were prepared by growing bacterial cultures (four replicates per strain) to mid-log phase (optical density at 600 nm [OD_{600}], approximately 0.4 to 0.45) in HI medium and then a 50-μl aliquot from each culture was centrifuged for 2 min at 12,000 $\times$ *g* and the pelleted cells were resuspended in 1 ml solution A containing Na phosphate buffer (5 mM, pH 7.0) and dilute (20%) HI medium. A 25-μl aliquot of 0 μM or 5 μM cathelicidin-2 was added to the appropriate wells of a 96-well polypropylene tray and mixed gently with 25 μl of the cell suspension described above containing approximately 1×10^5 CFU of *P. multocida* cells and then incubated at 37°C for 3 h. To determine the number of viable cells in the assay, a sample of each starting cell suspension used in the assays, and a sample from each assay well, obtained before and after incubation, was serially diluted in 0.9% NaCl and then 100 μl of each dilution was plated onto HI agar and the plates were incubated overnight at 37°C. CFU were then enumerated, and the percentage of survival for each *P. multocida* strain was calculated by dividing the number of CFU per milliliter recovered following incubation with 2.5 μM cathelicidin-2 at 37°C for 3 h by the number of CFU recovered from the control assay (0 μM cathelicidin-2). Statistical differences between experiments were calculated using an unpaired *t* test with Welch's correction (Graphpad Prism).

Chicken virulence trials. The virulence of the *petL* and *petK* VP161 Targetron mutants (AL1354 and AL2577) relative to the virulence of wild-type parent strain VP161 was determined using groups of 10 Hy-Line Brown chickens (approximately 14 weeks of age). Two routes of infection were employed: an intramuscular (i.m.) route and an intratracheal (i.t.) route (to mimic the natural route of infection). For the i.m. route, approximately 1×10^3 CFU of *P. multocida* in 100 μl HI medium was injected into the left pectoral muscle using a 23-gauge needle. For the i.t. route, birds were carefully restrained with the beak held open, allowing approximately 1×10^7 CFU in 100 μl HI medium of *P. multocida* to be delivered into the open trachea using a silicone-sleeved, blunt-ended, 18-gauge needle. Viable counts of each culture used for challenge were determined by serial dilution followed by enumeration on HI agar. Following i.m. or i.t. challenge, all birds were observed hourly from 13 h postchallenge until the end of the experiment for signs of fowl cholera and euthanized when deemed incapable of survival. All animal work was performed with the approval of the relevant animal ethics committee.

High-throughput RNA sequencing. High-throughput RNA sequencing was performed on RNA extracted and purified from *P. multocida* wild-type strain VP161 and the VP161 *fis* mutant (AL1405). Each strain was grown in HI broth (in duplicate), and samples were taken for RNA extraction during the early exponential growth phase (OD_{600} = 0.2), the mid-exponential growth phase ($OD_{600\ nm}$ = 0.4), and the late-exponential growth phase (OD_{600} = 0.6). RNA was extracted and purified, rRNA was depleted, and cDNA libraries were prepared, validated, and normalized as described previously (37). Libraries were sequenced and mapped to the draft VP161 genome as described previously (53). Genes examined in this study were identified as being differentially expressed if they displayed a $\geq$1.0 $\log_2$ ($\geq$2.0-fold) change in expression across the duplicate samples at a FDR of $\leq$0.05.

SUPPLEMENTAL MATERIAL

Supplemental material for this article may be found at https://doi.org/10.1128/IAI.00557-17.

SUPPLEMENTAL FILE 1, PDF file, 0.4 MB.

ACKNOWLEDGMENTS

We thank Jacek Stupak at the National Research Council, Canada, for MS support. We also thank Jennifer Steen and Marietta John at Monash University for the construction of strain AL1354 and for assistance during the chicken virulence trials, respectively.

This study was funded in part by the Australian Research Council, Canberra, Australia.

REFERENCES

1. Wilkie IW, Harper M, Boyce JD, Adler B. 2012. *Pasteurella multocida*: diseases and pathogenesis. Curr Top Microbiol Immunol 361:1–22.
2. Wilson BA, Ho M. 2013. *Pasteurella multocida*: from zoonosis to cellular microbiology. Clin Microbiol Rev 26:631–655. https://doi.org/10.1128/CMR.00024-13.
3. St Michael F, Li J, Vinogradov E, Larocque S, Harper M, Cox AD. 2005. Structural analysis of the lipopolysaccharide of *Pasteurella multocida* strain VP161: identification of both Kdo-P and Kdo-Kdo species in the lipopolysaccharide. Carbohydr Res 340:59–68. https://doi.org/10.1016/j.carres.2004.10.017.
4. Harper M, John M, Turni C, Edmunds M, St Michael F, Adler B, Blackall PJ, Cox AD, Boyce JD. 2015. Development of a rapid multiplex PCR assay to genotype *Pasteurella multocida* strains by use of the lipopolysaccharide outer core biosynthesis locus. J Clin Microbiol 53:477–485. https://doi.org/10.1128/JCM.02824-14.
5. Harper M, St Michael F, John M, Vinogradov E, Steen JA, van Dorsten L, Steen JA, Turni C, Blackall PJ, Adler B, Cox AD, Boyce JD. 2013. *Pasteurella multocida* Heddleston serovar 3 and 4 strains share a common lipopolysaccharide biosynthesis locus but display both inter- and intrastrain lipopolysaccharide heterogeneity. J Bacteriol 195:4854–4864. https://doi.org/10.1128/JB.00779-13.
6. DeAngelis PL, Jing W, Drake RR, Achyuthan AM. 1998. Identification and molecular cloning of a unique hyaluronan synthase from *Pasteurella multocida*. J Biol Chem 273:8454–8458. https://doi.org/10.1074/jbc.273.14.8454.
7. Harper M, Cox AD, Adler B, Boyce JD. 2011. *Pasteurella multocida* lipopolysaccharide: the long and the short of it. Vet Microbiol 153:109–115. https://doi.org/10.1016/j.vetmic.2011.05.022.
8. Harper M, Cox AD, St Michael F, Wilkie IW, Boyce JD, Adler B. 2004. A heptosyltransferase mutant of *Pasteurella multocida* produces a truncated lipopolysaccharide structure and is attenuated in virulence. Infect Immun 72:3436–3443. https://doi.org/10.1128/IAI.72.6.3436-3443.2004.
9. Boyce JD, Harper M, Wilkie IW, Adler B. 2010. *Pasteurella*, p 325–346. *In* Gyles CL, Prescott JF, Songer JG, Thoen CO (ed), Pathogenesis of bacterial infections of animals, 4th ed. Blackwell Publishing, Ames, IA.
10. St Michael F, Li J, Cox AD. 2005. Structural analysis of the core oligosaccharide from *Pasteurella multocida* strain X73. Carbohydr Res 340:1253–1257. https://doi.org/10.1016/j.carres.2005.02.014.
11. Cox AD, Wright JC, Li J, Hood DW, Moxon ER, Richards JC. 2003. Phosphorylation of the lipid a region of meningococcal lipopolysaccharide: identification of a family of transferases that add phosphoethanolamine to lipopolysaccharide. J Bacteriol 185:3270–3277. https://doi.org/10.1128/JB.185.11.3270-3277.2003.
12. Wright JC, Hood DW, Randle GA, Makepeace K, Cox AD, Li J, Chalmers R, Richards JC, Moxon ER. 2004. *lpt6*, a gene required for addition of phosphoethanolamine to inner-core lipopolysaccharide of *Neisseria meningitidis* and *Haemophilus influenzae*. J Bacteriol 186:6970–6982. https://doi.org/10.1128/JB.186.20.6970-6982.2004.
13. St Michael F, Harper M, Parnas H, John M, Stupak J, Vinogradov E, Adler B, Boyce JD, Cox AD. 2009. Structural and genetic basis for the serological differentiation of *Pasteurella multocida* Heddleston serotypes 2 and 5. J Bacteriol 191:6950–6959. https://doi.org/10.1128/JB.00787-09.
14. Mackinnon FG, Cox AD, Plested JS, Tang CM, Makepeace K, Coull PA, Wright JC, Chalmers R, Hood DW, Richards JC, Moxon ER. 2002. Identification of a gene (*lpt-3*) required for the addition of phosphoethanolamine to the lipopolysaccharide inner core of *Neisseria meningitidis* and its role in mediating susceptibility to bactericidal killing and opsonophagocytosis. Mol Microbiol 43:931–943. https://doi.org/10.1046/j.1365-2958.2002.02754.x.
15. Wanty C, Anandan A, Piek S, Walshe J, Ganguly J, Carlson RW, Stubbs KA, Kahler CM, Vrielink A. 2013. The structure of the neisserial lipooligosaccharide phosphoethanolamine transferase A (LptA) required for resistance to polymyxin. J Mol Biol 425:3389–3402. https://doi.org/10.1016/j.jmb.2013.06.029.
16. Stojanoski V, Sankaran B, Prasad BV, Poirel L, Nordmann P, Palzkill T. 2016. Structure of the catalytic domain of the colistin resistance enzyme MCR-1. BMC Biol 14:81. https://doi.org/10.1186/s12915-016-0303-0.
17. Hu M, Guo J, Cheng Q, Yang Z, Chan EW, Chen S, Hao Q. 2016. Crystal structure of *Escherichia coli* originated Mcr-1, a phosphoethanolamine transferase for colistin resistance. Sci Rep 6:38793. https://doi.org/10.1038/srep38793.
18. Fage CD, Brown DB, Boll JM, Keatinge-Clay AT, Trent MS. 2014. Crystallographic study of the phosphoethanolamine transferase EptC required for polymyxin resistance and motility in *Campylobacter jejuni*. Acta Crystallogr D Biol Crystallogr 70:2730–2739. https://doi.org/10.1107/S1399004714017623.
19. Cullen TW, Trent MS. 2010. A link between the assembly of flagella and lipooligosaccharide of the Gram-negative bacterium *Campylobacter jejuni*. Proc Natl Acad Sci U S A 107:5160–5165. https://doi.org/10.1073/pnas.0913451107.
20. Cullen TW, Madsen JA, Ivanov PL, Brodbelt JS, Trent MS. 2012. Characterization of unique modification of flagellar rod protein FlgG by *Campylobacter jejuni* lipid A phosphoethanolamine transferase, linking bacterial locomotion and antimicrobial peptide resistance. J Biol Chem 287:3326–3336. https://doi.org/10.1074/jbc.M111.321737.
21. Cullen TW, O'Brien JP, Hendrixson DR, Giles DK, Hobb RI, Thompson SA, Brodbelt JS, Trent MS. 2013. EptC of *Campylobacter jejuni* mediates phenotypes involved in host interactions and virulence. Infect Immun 81:430–440. https://doi.org/10.1128/IAI.01046-12.
22. Bontemps-Gallo S, Cogez V, Robbe-Masselot C, Quintard K, Dondeyne J, Madec E, Lacroix JM. 2013. Biosynthesis of osmoregulated periplasmic glucans in *Escherichia coli*: the phosphoethanolamine transferase is encoded by *opgE*. BioMed Res Int 2013:371429. https://doi.org/10.1155/2013/371429.
23. Naessan CL, Egge-Jacobsen W, Heiniger RW, Wolfgang MC, Aas FE, Rohr A, Winther-Larsen HC, Koomey M. 2008. Genetic and functional analyses of PptA, a phospho-form transferase targeting type IV pili in *Neisseria gonorrhoeae*. J Bacteriol 190:387–400. https://doi.org/10.1128/JB.00765-07.
24. Trombley MP, Post DM, Rinker SD, Reinders LM, Fortney KR, Zwickl BW, Janowicz DM, Baye FM, Katz BP, Spinola SM, Bauer ME. 2015. Phosphoethanolamine transferase LptA in *Haemophilus ducreyi* modifies lipid A and contributes to human defensin resistance *in vitro*. PLoS One 10:e0124373. https://doi.org/10.1371/journal.pone.0124373.
25. Logan SM, Chen W, Aubry A, Gidney MA, Lacelle S, St Michael F, Kuolee R, Higgins M, Neufeld S, Cox AD. 2006. Production of a D-glycero-D-manno-heptosyltransferase mutant of *Mannheimia haemolytica* displaying a veterinary pathogen specific conserved LPS structure; development and functionality of antibodies to this LPS structure. Vet Microbiol 116:175–186. https://doi.org/10.1016/j.vetmic.2006.04.024.
26. Anwar MA, Choi S. 2014. Gram-negative marine bacteria: structural features of lipopolysaccharides and their relevance for economically important diseases. Mar Drugs 12:2485–2514. https://doi.org/10.3390/md12052485.
27. Månsson M, Hood DW, Li J, Richards JC, Moxon ER, Schweda EK. 2002. Structural analysis of the lipopolysaccharide from nontypeable *Haemophilus influenzae* strain 1003. Eur J Biochem 269:808–818. https://doi.org/10.1046/j.0014-2956.2001.02707.x.
28. Chatterjee SN, Chaudhuri K. 2003. Lipopolysaccharides of *Vibrio cholerae*. I. Physical and chemical characterization. Biochim Biophys Acta 1639:65–79. https://doi.org/10.1016/j.bbadis.2003.08.004.
29. Harper M, Boyce JD, Cox AD, St Michael F, Wilkie IW, Blackall PJ, Adler B. 2007. *Pasteurella multocida* expresses two lipopolysaccharide glycoforms simultaneously, but only a single form is required for virulence: identification of two acceptor-specific heptosyl I transferases. Infect Immun 75:3885–3893. https://doi.org/10.1128/IAI.00212-07.
30. Miller VL, Mekalanos JJ. 1988. A novel suicide vector and its use in construction of insertion mutations: osmoregulation of outer membrane proteins and virulence determinants in *Vibrio cholerae* requires *toxR*. J Bacteriol 170:2575–2583. https://doi.org/10.1128/jb.170.6.2575-2583.1988.
31. Steen JA, Steen JA, Harrison P, Seemann T, Wilkie I, Harper M, Adler B, Boyce JD. 2010. Fis is essential for capsule production in *Pasteurella multocida* and regulates expression of other important virulence factors. PLoS Pathog 6:e1000750. https://doi.org/10.1371/journal.ppat.1000750.
32. Wilkie IW, Grimes SE, O'Boyle D, Frost AJ. 2000. The virulence and protective efficacy for chickens of *Pasteurella multocida* administered by different routes. Vet Microbiol 72:57–68. https://doi.org/10.1016/S0378-1135(99)00187-X.
33. Heddleston KL. 1962. Studies on pasteurellosis. v. Two immunogenic types of *Pasteurella multocida* associated with fowl cholera. Avian Dis 6:315–321.
34. Cárdenas M, Fernández de Henestrosa AR, Campoy S, Perez de Rozas

AM, Barbé J, Badiola I, Llagostera M; Molecular Microbiology Group. 2001. Virulence of *Pasteurella multocida recA* mutants. Vet Microbiol 80:53–61. https://doi.org/10.1016/S0378-1135(00)00372-2.
35. van Dijk A, Veldhuizen EJ, Kalkhove SI, Tjeerdsma-van Bokhoven JL, Romijn RA, Haagsman HP. 2007. The beta-defensin gallinacin-6 is expressed in the chicken digestive tract and has antimicrobial activity against food-borne pathogens. Antimicrob Agents Chemother 51:912–922. https://doi.org/10.1128/AAC.00568-06.
36. Harper M, Cox A, St Michael F, Parnas H, Wilkie I, Blackall PJ, Adler B, Boyce JD. 2007. Decoration of *Pasteurella multocida* lipopolysaccharide with phosphocholine is important for virulence. J Bacteriol 189:7384–7391. https://doi.org/10.1128/JB.00948-07.
37. Mégroz M, Kleifeld O, Wright A, Powell D, Harrison P, Adler B, Harper M, Boyce JD. 2016. The RNA-binding chaperone Hfq is an important global regulator of gene expression in *Pasteurella multocida* and plays a crucial role in production of a number of virulence factors, including hyaluronic acid capsule. Infect Immun 84:1361–1370. https://doi.org/10.1128/IAI.00122-16.
38. Raetz CR, Whitfield C. 2002. Lipopolysaccharide endotoxins. Annu Rev Biochem 71:635–700. https://doi.org/10.1146/annurev.biochem.71.110601.135414.
39. Hegge FT, Hitchen PG, Aas FE, Kristiansen H, Lovold C, Egge-Jacobsen W, Panico M, Leong WY, Bull V, Virji M, Morris HR, Dell A, Koomey M. 2004. Unique modifications with phosphocholine and phosphoethanolamine define alternate antigenic forms of *Neisseria gonorrhoeae* type IV pili. Proc Natl Acad Sci U S A 101:10798–10803. https://doi.org/10.1073/pnas.0402397101.
40. Lewis LA, Choudhury B, Balthazar JT, Martin LE, Ram S, Rice PA, Stephens DS, Carlson R, Shafer WM. 2009. Phosphoethanolamine substitution of lipid A and resistance of *Neisseria gonorrhoeae* to cationic antimicrobial peptides and complement-mediated killing by normal human serum. Infect Immun 77:1112–1120. https://doi.org/10.1128/IAI.01280-08.
41. Trent MS. 2004. Biosynthesis, transport, and modification of lipid A. Biochem Cell Biol 82:71–86. https://doi.org/10.1139/o03-070.
42. Brabetz W, Muller-Loennies S, Holst O, Brade H. 1997. Deletion of the heptosyltransferase genes *rfaC* and *rfaF* in *Escherichia coli* K-12 results in an Re-type lipopolysaccharide with a high degree of 2-aminoethanol phosphate substitution. Eur J Biochem 247:716–724. https://doi.org/10.1111/j.1432-1033.1997.00716.x.
43. Cox AD, Brisson JR, Varma V, Perry MB. 1996. Structural analysis of the lipopolysaccharide from *Vibrio cholerae* O139. Carbohydr Res 290:43–58. https://doi.org/10.1016/0008-6215(96)00135-8.
44. Reynolds CM, Kalb SR, Cotter RJ, Raetz CR. 2005. A phosphoethanolamine transferase specific for the outer 3-deoxy-D-manno-octulosonic acid residue of *Escherichia coli* lipopolysaccharide. Identification of the *eptB* gene and Ca2+ hypersensitivity of an *eptB* deletion mutant. J Biol Chem 280:21202–21211.
45. Sun Q, Knirel YA, Lan R, Wang J, Senchenkova SN, Jin D, Shashkov AS, Xia S, Perepelov AV, Chen Q, Wang Y, Wang H, Xu J. 2012. A novel plasmid-encoded serotype conversion mechanism through addition of phosphoethanolamine to the O-antigen of *Shigella flexneri*. PLoS One 7:e46095. https://doi.org/10.1371/journal.pone.0046095.
46. Klein G, Muller-Loennies S, Lindner B, Kobylak N, Brade H, Raina S. 2013. Molecular and structural basis of inner core lipopolysaccharide alterations in *Escherichia coli*: incorporation of glucuronic acid and phosphoethanolamine in the heptose region. J Biol Chem 288:8111–8127. https://doi.org/10.1074/jbc.M112.445981.
47. Knirel YA, Widmalm G, Senchenkova SN, Jansson PE, Weintraub A. 1997. Structural studies on the short-chain lipopolysaccharide of *Vibrio cholerae* O139 Bengal. Eur J Biochem 247:402–410. https://doi.org/10.1111/j.1432-1033.1997.00402.x.
48. Aas FE, Winther-Larsen HC, Wolfgang M, Frye S, Lovold C, Roos N, van Putten JP, Koomey M. 2007. Substitutions in the N-terminal alpha helical spine of *Neisseria gonorrhoeae* pilin affect Type IV pilus assembly, dynamics and associated functions. Mol Microbiol 63:69–85. https://doi.org/10.1111/j.1365-2958.2006.05482.x.
49. Tzeng YL, Datta A, Ambrose K, Lo M, Davies JK, Carlson RW, Stephens DS, Kahler CM. 2004. The MisR/MisS two-component regulatory system influences inner core structure and immunotype of lipooligosaccharide in *Neisseria meningitidis*. J Biol Chem 279:35053–35062. https://doi.org/10.1074/jbc.M401433200.
50. Boyce JD, Cullen PA, Adler B. 2004. Genomic-scale analysis of bacterial gene and protein expression in the host. Emerg Infect Dis 10:1357–1362. https://doi.org/10.3201/eid1008.031036.
51. Chromek M, Slamova Z, Bergman P, Kovacs L, Podracka L, Ehren I, Hokfelt T, Gudmundsson GH, Gallo RL, Agerberth B, Brauner A. 2006. The antimicrobial peptide cathelicidin protects the urinary tract against invasive bacterial infection. Nat Med 12:636–641. https://doi.org/10.1038/nm1407.
52. Murray GL, Ellis KM, Lo M, Adler B. 2008. *Leptospira interrogans* requires a functional heme oxygenase to scavenge iron from hemoglobin. Microbes Infect 10:791–797. https://doi.org/10.1016/j.micinf.2008.04.010.
53. Henry R, Crane B, Powell D, Deveson Lucas D, Li Z, Aranda J, Harrison P, Nation RL, Adler B, Harper M, Boyce JD, Li J. 2015. The transcriptomic response of *Acinetobacter baumannii* to colistin and doripenem alone and in combination in an in vitro pharmacokinetics/pharmacodynamics model. J Antimicrob Chemother 70:1303–1313. https://doi.org/10.1093/jac/dku536.